X-625-73-290
PREPRINT

NASA TM X- 70476

NIGHTTIME ION COMPOSITION MEASUREMENTS AT THE GEOMAGNETIC EQUATOR

R. A. GOLDBERG
A. C. AIKIN

OCTOBER 1973

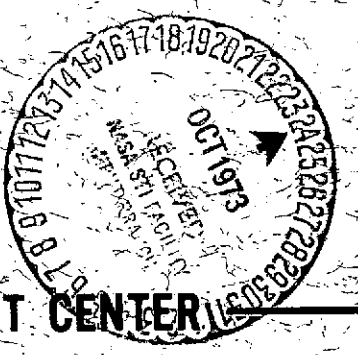

GSFC
GODDARD SPACE FLIGHT CENTER
GREENBELT, MARYLAND

NIGHTTIME ION COMPOSITION MEASUREMENTS AT THE GEOMAGNETIC EQUATOR

by

R. A. Goldberg
A. C. Aikin
Laboratory for Planetary Atmospheres
NASA/Goddard Space Flight Center
Greenbelt, Maryland

ABSTRACT

Two ion composition profiles, representative of the nighttime equatorial ionosphere between 90 km and 300 km, are presented. These profiles were obtained by two rocket-borne ion mass spectrometers on a single night for solar zenith angles of 112° and 165°. For both flights, the principal ion above 200 km is O^+. The downward drift of the atomic ions O^+ and N^+, coinciding with the post-sunset lowering of the F2 peak, is observed through an enhancement of the density of O^+ at altitudes above 200 km and N^+ above 240 km. Below the drift region, O^+ and N^+ are observed in concentrations larger than expected. The NO^+ altitude distribution retains its shape throughout the night, and below 210 km, is the principal ion. The behavior of O_2^+ can be explained by the O^+, electron density and theoretical neutral nitric oxide concentrations. Light metallic ions, including Mg^+, Na^+, and possibly Si^+, are observed to altitudes approaching 300 km and are affected by vertical drift.

INTRODUCTION

At the magnetic equator the F region exhibits a vertical drift which is correlated with E region dynamo electric fields. Rocket studies of electron density (Aikin and Blumle, 1968) and incoherent backscatter soundings (Farley, 1966; Balsley, 1973) have demonstrated that at night the equatorial F region moves downward enhancing the lower F region ionosphere above that predicted on the basis of maintenance by scattered solar ultraviolet radiations. A detailed description of the behavior of the nighttime equatorial ionosphere has not been possible because information on the changes of ion composition at lower altitudes during the course of the night has not been available.

In this work we present two measurements of positive ion composition from 90 to 300 km altitude. These profiles were obtained during the night of March 9-10, 1970 with ion mass spectrometers launched from the Indian Thumba Equatorial Rocket Launch Site (TERLS) located at 8.53°N latitude, 76.95°E longitude, and -1.7° magnetic dip. The first launching, rocket 18.97, occurred at a solar zenith angle of 112° (1938 LMT) and reached an apogee of 298 km. At this time, the F2 peak had reached maximum height, which was in excess of 500 km. The second measurement, rocket 18.98, was launched at $\chi = 165^{\circ}$, five and one-half hours later (0108 LMT) and following the downward drift of the F region peak to an altitude of approximately 300 km. Transport of the F region

during this period was determined from analysis of the ionograms taken at frequent intervals.

A third rocket (18.99) launched 35 minutes after 18.98, carried instrumentation to measure untraviolet radiations important for the maintenance of the nighttime ionosphere. The details and results of these experiments are discussed elsewhere (Paresce et al, 1973a, 1973b).

INSTRUMENTATION AND ANALYSIS

Each payload underwent nose cone ejection and separation from the rocket motor prior to ion composition sampling. Characteristics of the flights of 18.97 and 18.98 are given in Aikin and Goldberg (1973). Trajectories were determined using a tone range/telemetry interferometer tracking system (Hudgins and Lease, 1967). Magnetometers were used to provide rocket-magnetic field angles. Payload aspects for both well behaved flights were then determined by assuming the payloads to lie in the trajectory plane.

The ion composition was measured using pumped, quadrupole ion mass spectrometers of the type discussed in Goldberg and Aikin, 1971. The characteristics of each spectrometer are tabulated in Table 1. In addition to ion mass spectrometers, the payloads for rockets 18.97 and 18.98 contained instrumentation to measure positive ion and electron densities. Total electron density was obtained using the continuous wave dispersive Doppler technique (Sedden, 1953; Bauer and Jackson,

1962) at transmitting frequencies of 73.6 and 24.53 MHz. Quasi-longitudinal propagation conditions were preserved at the magnetic equator by launching in a southward direction.

Sample mass spectra and the method of data analysis for these rockets are given in Aikin and Goldberg (1973). The total ion spectrometer current was normalized to the electron density profile obtained by the propagation experiment. Corrections for relative mass effects were applied from free molecular flow theory as discussed in Goldberg and Blumle (1970). The temperature profiles used to make these corrections were deduced from the U.S. Standard Atmosphere, 1966 Supplement.

Above 180 km and only on the flight of 18.98, a significant background was superimposed on the spectra. It increased three orders of magnitude by apogee, masking the minor constituents in the upper domains of the flight. The source of this background can be caused by soft energetic electrons in the 2 to 15 Kev energy range, with fluxes similar to those deduced by Heikkila (1971) at higher altitudes. The nature of this background source will be discussed elsewhere; it suffices here to state that the background currents were subtracted from the ion spectral currents to arrive at values used for normalization.

GEOPHYSICAL CONDITIONS

Figure 1 illustrates the variation of the F2 layer during the night of March 9-10, 1970, when the rocket

firings occurred. These data were obtained from ionogram studies. The ionogram true height analysis was optimized by fitting the low frequency ionogram data with the CW Doppler profile from 18.98. This fit and resulting low density slope was then applied to other ionograms during the night under the assumption that the low density slope remained unchanged.

It should be noted that the night of March 9-10, 1970 occurred after the great magnetic storm of March 8. On the night of March 9-10, the K index fluctuated between 4 and 6 indicating a period of moderate activity. Chandra and Rastogi (1972) have shown an inverse correlation between range blanketing spread F and K index at the magnetic equator under nighttime conditions. Hence, the moderate magnetic activity of March 9-10, 1970 correlates with the partial observation of the F region ionogram traces observed, and permitted true height analysis from the ionograms for that night.

The upper part of Figure 1 illustrates the variation of two constant density profiles, one near the minimum ($N_e = 5 \times 10^4 cm^{-3}$) and one near the maximum ($N_e = 4 \times 10^5 cm^{-3}$) value for the F2 layer. We note that both portions of the layer moved downward at the same rate implying a preservation of the layer shape during this motion, as argued by Balsley (1969). The slope of the curve depicts the change of isopleth altitude with time and can be used to derive

the vertical velocity profile. This is shown in the lower half of Figure 1.

The velocity profile obtained for Thumba exhibits many of the properties observed at Jicamarca, Peru (Balsley, 1973). There was a post-sunset upward drift followed by a more sustained downward drift. The drift magnitude had decreased substantially by midnight. The launch sequence of the rockets, also indicated in Figure 1, shows the first measurement to have occurred at a time when the F2 peak was near an altitude 550 km and undergoing an upward drift, while the second measurement occurred after the F2 layer had dropped to 300 km altitude. The downward drift was negligible at the time of the second measurement.

TOTAL ELECTRON DENSITY RESULTS

The profiles labelled N_i in Figure 2 are obtained from the CW propagation electron density experiment aboard each rocket. The results were verified by direct comparison with ionogram true height profiles determined for the launch time periods.

Below 200 km on both flights, N_i oscillates about a mean of approximately $2 \times 10^3 cm^{-3}$. On 18.98, N_i is seen to be greatly enhanced above this height, illustrating the downward transport of the F2 layer from its early post-sunset location well above the apogee of 18.97.

Returning to Figure 2, we note a certain amount of structure present in the N_i profile above 260 km on the

18.98 data but absent on the 18.97 profile. Rocket 18.97 was fired prior to any appearance of spread F on the ionograms, whereas 18.98 launch time time ionograms showed a weak range spread F condition. Hence the structure observed may be associated with this equatorial phenomenon.

Finally, we note the lower altitude oscillations in N_i present for both flights. No explanation for this observation exists at present although they may possibly be associated with tidal motions or with an unknown nighttime source of ionization near the 140 km level.

ION COMPOSITION RESULTS

Figures 2 and 3 compare the time behavior of the nonmetallic and metallic ions respectively. The quantity N_i refers to the total ion density profile, which is equivalent to electron density through charge neutrality considerations. The most noticeable feature of the profiles is the effect of downward transport of atomic ions and electrons, which can be interpreted in terms of the velocity time profile shown in Figure 1. The first measurement was made during a period of upward drift. This was followed by a period of downward drift, during which the O^+ concentration at 300 km increased nearly three orders of magnitude. Below 200 km the O^+ concentration decreased between the two measurements, less rapidly than would be expected from the known nighttime production sources.

There is a measureable concentration of N^+ observed although the altitude distribution differs between the two flights. The earlier flight exhibits a nearly altitude independent distribution of about 20 ions/cm^3. During the flight of 18.98, N^+ assumed a distribution that increased near apogee but decreased below 240 km with respect to the 18.97 distribution. The 18.98 altitude variation of N^+ paralleled that of O^+ but with a reduced abundance.

While drift effects control the number and species distribution of ions above 200 km, drift could not be expected to be important below 200 km, where the time constant for the loss of both O^+ and N^+ is very short and the major ions observed are molecular, i.e. NO^+ and O_2^+. These ions are considered to be maintained by scattered solar radiation (Ogawa and Tohmatsu, 1966; Keneshea et al., 1970; and Fujitaka et al., 1971).

The sources of scattered radiation, which have been proposed as ionizing radiations, include Lyman alpha for NO, Lyman beta for O_2, and the HeI and HeII radiations at 584A and 304A, which can ionize most atmospheric constituents. The Lyman alpha and beta radiations can only be responsible for the distribution below 130 km (Aikin and Goldberg, 1973). The HeI and HeII radiations, having a peak ionization rate between 150 and 200 km, were measured on a third rocket, 18.99, launched 35 minutes after 18.98. Fluxes of 16R for 584A and 8R for 304A were obtained (Paresce, 1973a, b).

These values are larger than the 10R for 584A and 1R for 304A used in computations of the nighttime ionosphere, e.g. by Fujitaka et al. (1971), but the enhanced radiation measured does not modify the computed NO^+ and O_2^+ densities significantly below 180 km. The observations indicate that above this altitude the NO^+ and O_2^+ distributions become increasingly sensitive to the drift of atomic ions.

The presence of O^+ and N^+ below 200 km cannot be explained solely by the scattered radiations discussed above. These radiations would account for at most, 30 O^+ ions/cm^3 at 180 km and a factor of ten less at 150 km for the zenith angle ($\chi = 165^\circ$) of 18.98. For O^+, either another source of ionization and/or a small rate coefficient for the charge exchange reaction involving O^+ and O_2^+ is required. The situation is similar for N^+. Mechanisms for the production of N^+ include direct photoionization, dissociative ionization of N_2 and charge exchange between N_2^+ and N (Rishbeth et al., 1972). At night the primary source is photoionization by scattered solar EUV. This source is directly dependent on the atomic nitrogen content in the lower thermosphere. Additional production of N^+ by charge exchange between N_2^+ and N requires that the 28^+ observed be identified as N_2^+ rather than Si^+.

During both measurements 28^+ was observed in quantity. This constituent is shown on both Figure 2 (non-metallic constituents) and Figure 3 (metallic constituents) because

of probable and indistinguishable contributions from N_2^+ and Si^+. Typical values shown range between 10 and 50 ions/cm^3. If 28^+ is identified as N_2^+, then it is difficult to explain the nighttime maintenance of this ion. The ion should be lost by ion-neutral reactions involving O and O_2. The nighttime scattered helium radiations account for, at their maximum, between 0.1 and 0.5 ions/cm^3 sec. They provide no contribution below 150 km although 28^+ is observed below this height. Alternate possibilities include additional sources of ionization or the identification of 28^+ as Si^+. If Si^+, this constituent would have the typically long lifetime of atomic ions and be subject to a drift-controlled height structure. This last alternative is particularly attractive since reference to Figure 3 shows that 28^+ tracks the other metal ion distributions such as Mg^+.

Above 200 km the O_2^+ and NO^+ distributions are sensitive functions of O^+ drift. Enhancement of O^+ between the two flights increases the O_2^+ concentration by nearly an order of magnitude but there is less than a factor of 2 increase of NO^+. The slopes of the O_2^+ and NO^+ distributions do not coincide for 18.97 but are essentially the same for 18.98.

Above 200 km NO^+ is produced by the reaction between O^+ and N_2 (rate $\equiv k_1$). Dissociative recombination of NO^+ with electrons (rate $\equiv \alpha_{D1}$) is the loss process so that

under equilibrium conditions

$$NO^+ = \frac{k_1[O^+][N_2]}{\alpha_{D1} N_e} \cong \frac{k_1[N_2]}{\alpha_{D1}}$$

For the latter step, it is assumed that $O^+ \cong N_e$. A scale height can be derived which is indicative of the atmospheric temperature at the time of the flight. The profile of 18.98 rather than 18.97 is best suited for such analysis since the approximation is more accurate for nearly steady state conditions. The 18.98 data also show less scatter. The high altitude slope of the 18.98 NO^+ profile yields a scale height of 31.7 km. This is consistent with an exospheric temperature of 1200^oK and a model from the U.S. Standard Atmosphere (1966 Supplement) for this temperature can be adopted. This value can be favorably compared to the predicted exospheric temperature of approximately 1100^o for the geophysical conditions at the time of the flight. A value for k_1/α_{D1} of $(8\pm3)\times10^7$ derived from the measured NO^+ distribution is then obtained. If $\alpha_{D1} = 2\times10^{-7}$ (Bardsley, 1968), then $k_1 = (1.6\pm0.6)\times10^{-13}$ cm^3 sec^{-1}. Yonezawa (1970) has derived a value of 2×10^{-13} cm^3 sec^{-1} from ionospheric data and laboratory results give 5×10^{-13} cm^3 sec^{-1} at 600^oK (Dunkin et al., 1968). Finally, below 200 km the reaction $O_2^+ + NO \rightarrow NO^+ + O_2$ (rate = 6.3×10^{-10} $cm^3 sec$; Johnson et al., 1970) becomes increasingly more important as O^+ decreases, and must be considered.

The production of O_2^+ above 200 km is controlled by the reaction $O^+ + O_2 \rightarrow O_2^+ + O$ (rate $\equiv k_2$). Unlike NO^+, where loss is due solely to dissociative recombination (rate $\equiv \alpha_{D2}$), O_2^+ has an additional loss process represented by the charge exchange between O_2^+ and NO (rate $\equiv k_3$). One can write under equilibrium circumstances

$$[O_2^+] = \frac{k_2[O^+][O_2]}{\alpha_{D2}N_e + k_3[NO]}$$

For 18.98, $\chi = 165^o$, $O^+ \cong N_e$ and provided the second term in the denominator is negligible compared to the first above 240 km ([NO] be less than 10^{-3} $[N_2]$), an expression is derived which is similar to that for NO^+. The products $k_1[N_2]$ and $k_2[O_2]$ have nearly equal values leading to $[NO^+] \cong [O_2^+]$ in agreement with the observed data. In this instance O_2^+ charge exchange with NO is negligible in comparison with dissociative recombination.

The situation is more complicated for the flight of 18.97 when the solar zenith angle $\chi = 112^o$. In this instance there is an upward drift of O^+ and electrons. In addition there is a transition in the ionizing flux so that time variations must be considered in any detailed explanation of this profile.

Figure 3 compares the measured distribution of metal ions 28^+, Na^+; 24^+, Mg^+; 28^+, Si^+ or N_2^+; 39^+, K^+; and 40^+, Ca^+; for the two rocket flights. Typical spectra for the low altitude metallic ion data from flight 18.98 can be found in Aikin and Goldberg (1973).

Since neither spectrometer swept above mass 42, high pass filter mode data were employed to deduce information concerning heavier constituents. Following a technique outlined in Goldberg and Aikin (1971), high pass filter mode data for two AMU ranges ($1 \rightarrow \infty$; $32 \rightarrow \infty$) were used to deduce the relative sensitivity in this mode to the spectral mode. The T_B profile thus obtained represents all masses above 31^+ and is shown to 130 km. In the metallic belt between 90 and 100 km this is thought to be primarily Fe^+ (56^+), and above this height is O_2^+ (32^+). This latter conclusion is based on the result that at higher altitudes the T_B profile resembles O_2^+ during both flights.

As the comparison of the concentrated metallic ion peak height between 1938 and 0108 LMT illustrates, these long-lived atomic ions are affected by the electric field and exhibit a downward drift during the course of the night. However, the concentration does remain fixed in the presence of this drift. A detailed discussion of this problem can be found in Aikin and Goldberg (1973).

Above 200 km on both flights, the light metallic ions 23^+, 24^+ and 28^+ are observed in concentrations of $10/cm^3$. Heavier metallic constituents, represented by 39^+ and 40^+, are observed in much smaller quantities at altitudes above 100 km. Partial identification of T_B with Fe^+ leads to a similar result for this constituent also. The high altitude limits of these traces on 18.98 are not real, but caused by the background masking effect previously discussed.

The presence of light metallic ions at high altitudes (> 200 km) has previously been reported from rocket data at midlatitudes (Goldberg and Blumle, 1970) and satellite data (Taylor, 1973). These data would tend to suggest that long lived metallic ions are subject to ionospheric transport processes, and eventually disperse to regions far from their point of origin.

CONCLUSIONS

Two ion composition altitude profiles, representative of the behavior of the nighttime equatorial ionosphere, are presented. Between 200 and 300 km the dominant ion is O^+. This ion exhibits a nearly constant density of $2 \times 10^3 cm^{-3}$ for a zenith angle of 112^o. The F region exhibits a downward drift during the course of the night resulting in an increase in the concentration of O^+ by as much as a factor of 10^3 near 300 km. The O_2^+ concentration is correspondingly enhanced by O^+ charge exchange processes, due to the relative unimportance of O_2^+ loss by dissociative recombination and charge exchange with nitric oxide. The ion NO^+ exhibits little enhancement, consistent with theory. The ion N^+ exhibits some increase above 200 km, also caused by the downward drift.

Below 200 km N_e, O_2^+ and NO^+ remain nearly unchanged between flights. Below 160 km, O^+ and N^+ decrease too slowly to be accounted for by known loss processes, and

other sources of nighttime ionization are required. The constituent 28^+, if identified as N_2^+, is similarly over-abundant below 200 km, but if Si^+, can be suitably accounted for.

Light metal ions (Na^+, Mg^+, and possibly Si^+) are observed to altitudes of 300 km. Heavier metallics, such as Ca^+, K^+, and possibly Fe^+, the latter deduced from high pass filter mode data, are observed to 200 km but in reduced quantity. The metallic ions are apparently influenced by ionospheric transport processes, which at the equator result primarily in vertical drifting.

ACKNOWLEDGEMENTS

The results reported here were successfully obtained through the competent efforts of the Chemosphere Branch technical staff. In particular, we thank Messrs. Donald Silbert, Robert Farmer and Denis Endres for the development and preparation of the spectrometer flight package. Messrs. Roy Hagemeyer and Giles Spaid were largely responsible for the radio wave CW propagation experiment. We are indebted to Mr. John Jackson for his assistance in the interpretation of the ionosonde and CW propagation electron density data, and for his detailed trajectory analysis. We also thank the Indian Launch Range (TERLS) and the Goddard Sounding Rocket Division teams for their excellent cooperation and support.

TABLE

Spectrometer Characteristics for the instruments aboard payloads 18.97 and 18.98.

TABLE 1

CHARACTERISTIC	18.97	18.98
Entrance Aperture Diameter (mm)	0.74	0.74
Rod Length (mm)	101.6	101.6
Sampling Interval (sec)	1.56	1.69
Sweep Range (AMU)	1-42	1-41
Mass Range for High Pass Filter Mode, T_B (AMU)	~ 31	~ 31
Time/Unit Mass (sec/AMU)	.030	.034
RF Frequency (MHz)	2.85	2.85
Aperture Attraction Potential (volts)	- 10	- 10

FIGURES

Figure 1. (upper) F-region electron density isopleths as a function of time for the night of March 9-10, 1970. (lower) Vertical drift velocity as a function of time.

Figure 2. Observed distribution of positive, non-metallic ion species in the nighttime E and F regions over Thumba: (left) upleg of rocket flight 18.97 at 1938 LMT, $\chi = 112^{o}$; (right) upleg of rocket flight 18.98 at 0108 LMT, $\chi = 165^{o}$.

Figure 3. Observed distribution of positive metallic ion species in the nighttime E and F regions over Thumba: (left) 18.97; (right) 18.98.

REFERENCES

Aikin, A.C. and L.J. Blumle, "Rocket Measurements of the E Region Electron Concentration Distribution in the Vicinity of the Geomagnetic Equator", J. Geophys. Res., 73, 1617, 1968.

Aikin, A.C. and R.A. Goldberg, "Metallic Ions in the Equatorial Ionosphere", J. Geophys. Res., 78, 734, 1973.

Balsley, B.B., "Nighttime Electric Fields and Vertical Ionospheric Drifts Near the Magnetic Equator", J. Geophys. Res., 74, 1213, 1969.

Balsley, B.B., "Electric Fields in the Equatorial Ionosphere: A Review of Techniques and Measurements", J. Atmos. Terr. Phys., 35, 1035, 1973.

Bardsley, J.N., "The Theory of Dissociative Recombination", J. Phys., B1, 365, 1968.

Bauer, S.J. and J.E. Jackson, "Rocket Measurements of the Upper Atmosphere by a Radio Propagation Technique", J. Brit. IRE, 23, 139, 1962.

Chandra, H. and R.G. Rastogi, "Spread F at Magnetic Equatorial Station Thumba", Ann. Geophys., 28, 37, 1972.

Dunkin, D.B., F.C. Fehsenfeld, A.L. Schmeltekopf and E.E. Ferguson, "Ion-Molecule Reaction Studies from 300° to 600°K in a Temperature-Controlled Flowing Afterglow System", J. Chem. Phys., 49, 1365, 1968.

Farley, D.T., Jr., "Observations of the Equatorial Ionosphere Using Incoherent Backscatter" (p. 446), Electron Density Profiles in Ionosphere and Exosphere, ed. by Jon Frihagen, John Wiley and Sons Inc., New York, 1966.

Fujitaka, K., T. Ogawa and T. Tohmatsu, "A Numerical Computation of the Ionization Redistribution Effect of the Wind in the Nighttime Ionosphere", J. Atmos. Terr. Phys., 33, 687, 1971.

Goldberg, R.A. and L.J. Blumle, "Positive Ion Composition from a Rocket-Borne Mass Spectrometer", J. Geophys. Res., 75, 133, 1970.

Goldberg, R.A. and A.C. Aikin, "Studies of Positive Ion Composition in the Equatorial D Region Ionosphere", J. Geophys. Res., 76, 8352, 1971.

Heikkila, W.J., "Soft Particles Fluxes Near the Equator", J. Geophys. Res., 76, 1076, 1971.

Hudgins, J.I. and J.R. Lease, "Tone Range-Telemetry Tracking System for Support of Sounding Rocket Payloads", NASA Spec. Publ. 219, 1967.

Johnson, R., H.L. Brown and N.A. Biondi, "Ion-Molecule Reactions Involving N_2^+, N^+, O_2^+ and O^+ Ions from 300°K to ~ 1 ev", J. Chem. Phys., 52, 5080, 1970.

Keneshea, T.J., R.S. Narcisi and W. Swider, Jr., "Diurnal Model of the E Region", J. Geophys. Res., 75, 845, 1970.

Ogawa, T., and T. Tohmatsu, "Photoelectric Processes in the Upper Atmosphere. 2. The Hydrogen and Helium Ultraviolet Glow as an Origin of the Nighttime Ionosphere", Rept. Ionosphere Space Res. Japan, 20, 395, 1966.

Paresce, F., S. Boyer and S. Kumar, "Observations of the He II 304A Radiation in the Night Sky", J. Geophys. Res., 78, 71, 1973a.

Paresce, F., S. Boyer and S. Kumar, "Evidence for an Interstellar of Interplanetary Source of Diffuse HeI 584A Radiation", to be published Astrophys. J. Letters, 1973b.

Rishbeth, H., P. Bauer, and W.B. Hanson, "Molecular Ions in the F2 Layer", Planet. Space Sci., 20, 1287, 1972.

Sedden, J.C., "Propagation Measurements in the Ionosphere with the Aid of Rockets", J. Geophys. Res., 58, 323, 1953.

Taylor, H.A., Jr., "Parametric Description of Thermospheric Ion Composition Results", J. Geophys. Res., 78, 315, 1973.

U. S. Standard Atmosphere Supplements, U. S. Government Printing Office, 1966.

Yonezawa, T., "The Vertical Distribution of Ionization at the F2 Peak Related to Ionic Production and Transport Processes", Ann. Geophys., 26, 581, 1970.

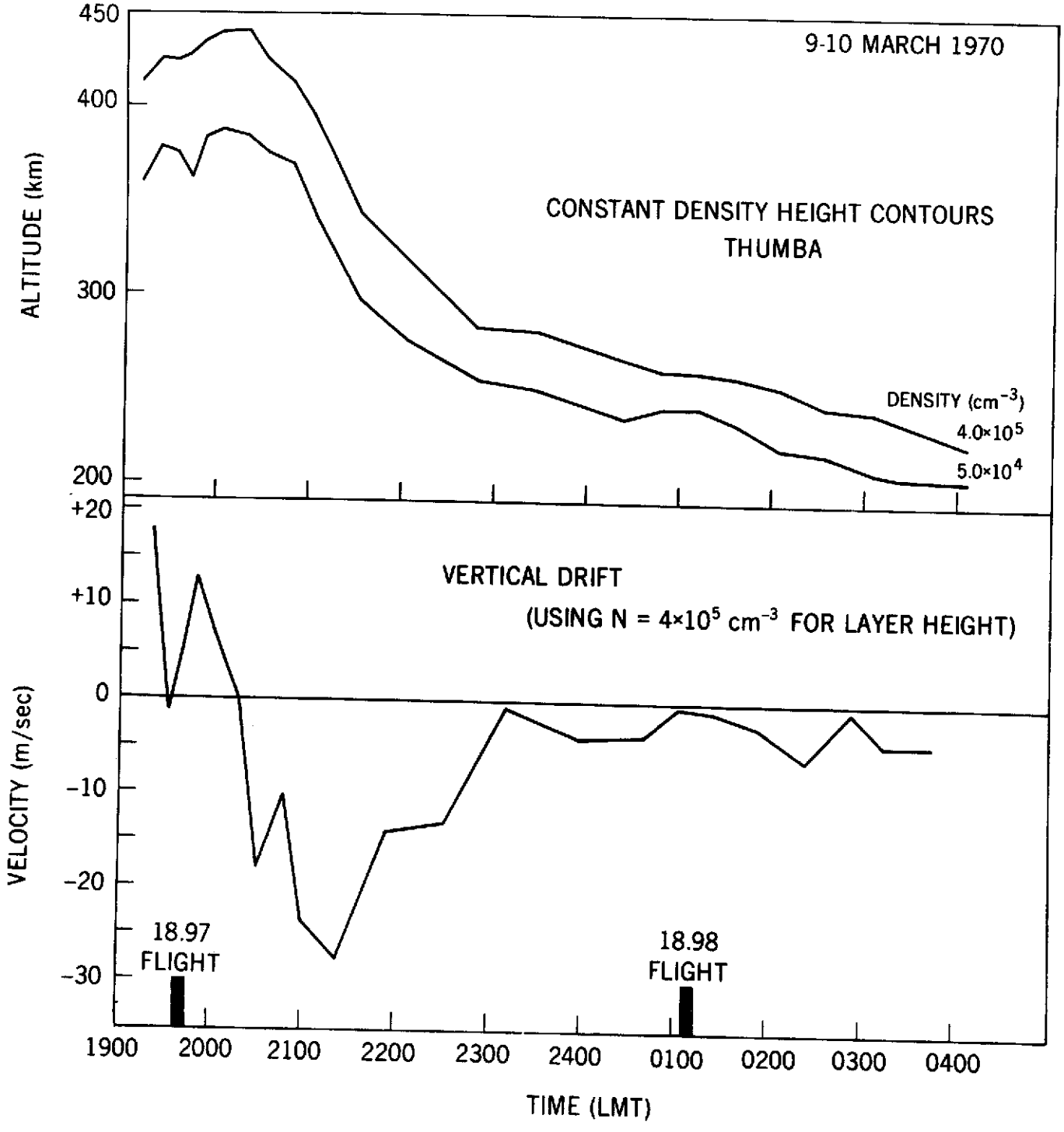
9-10 MARCH 1970
CONSTANT DENSITY HEIGHT CONTOURS
THUMBA
ALTITUDE (km)
450
400
300
200
DENSITY (cm^{-3})
4.0×10^5
5.0×10^4
VERTICAL DRIFT
(USING N = 4×10^5 cm^{-3} FOR LAYER HEIGHT)
VELOCITY (m/sec)
+20
+10
0
-10
-20
-30
18.97
FLIGHT
18.98
FLIGHT
1900
2000
2100
2200
2300
2400
0100
0200
0300
0400
TIME (LMT)

Figure 1

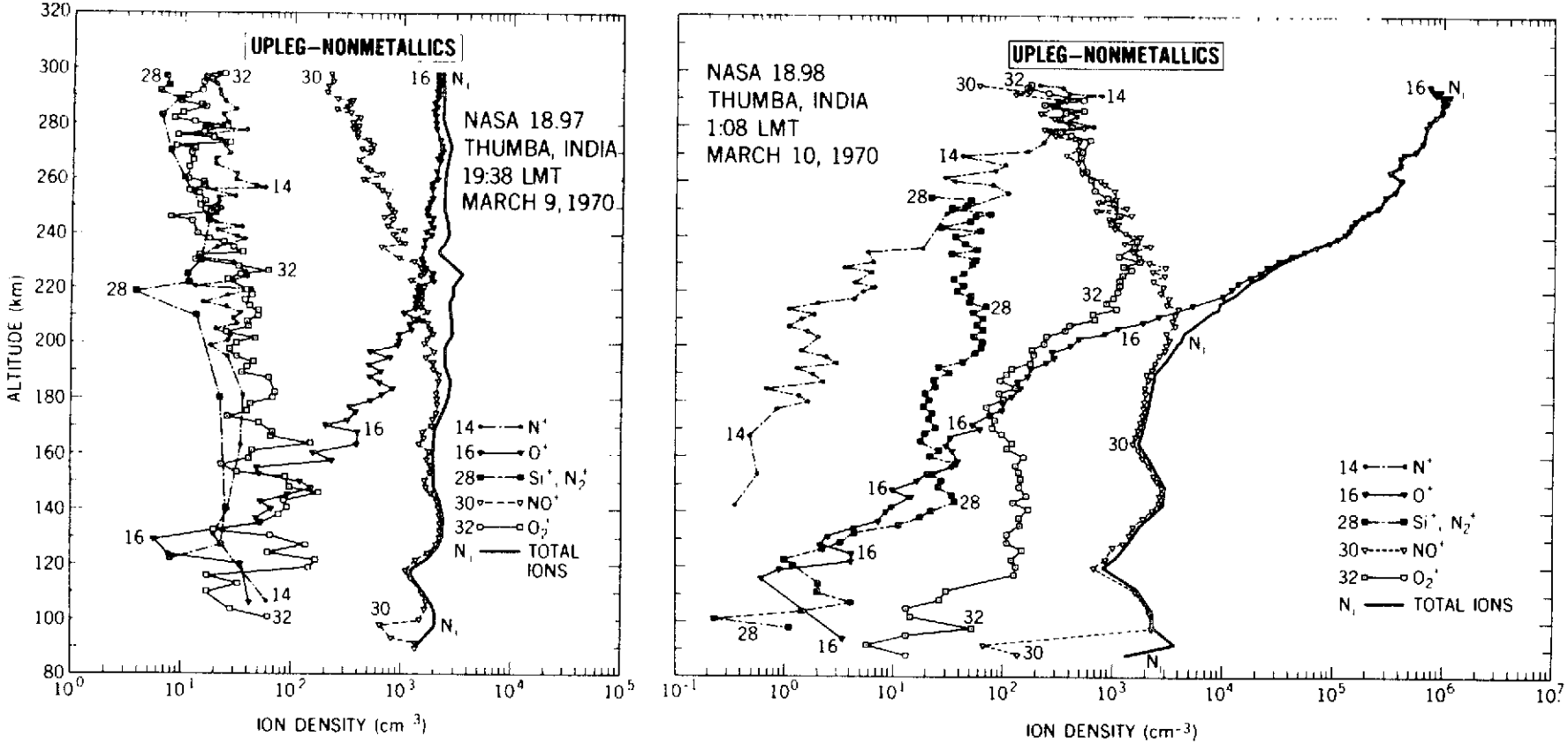
UPLEG–NONMETALLICS
NASA 18.97
THUMBA, INDIA
19:38 LMT
MARCH 9, 1970
14 N+
16 O+
28 Si+, N2+
30 NO+
32 O2+
N1 TOTAL IONS
ALTITUDE (km)
ION DENSITY (cm-3)
UPLEG–NONMETALLICS
NASA 18.98
THUMBA, INDIA
1:08 LMT
MARCH 10, 1970
14 N+
16 O+
28 Si+, N2+
30 NO+
32 O2+
N1 TOTAL IONS
ION DENSITY (cm-3)

Figure 2

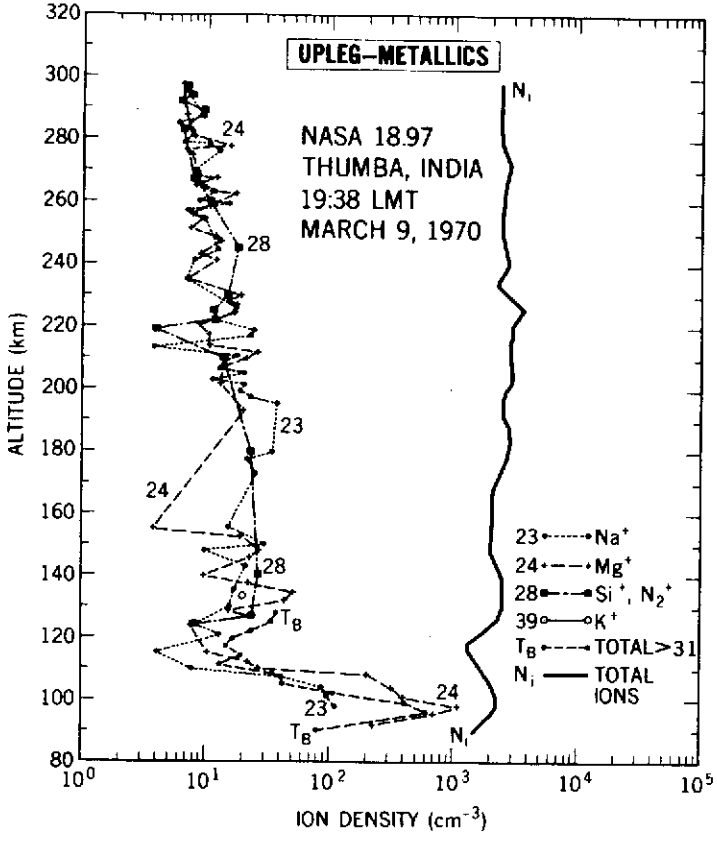
UPLEG–METALLICS
NASA 18.97
THUMBA, INDIA
19:38 LMT
MARCH 9, 1970
ALTITUDE (km)
ION DENSITY (cm⁻³)
23 Na⁺
24 Mg⁺
28 Si⁺, N₂⁺
39 K⁺
T_B TOTAL>31
N_i TOTAL IONS

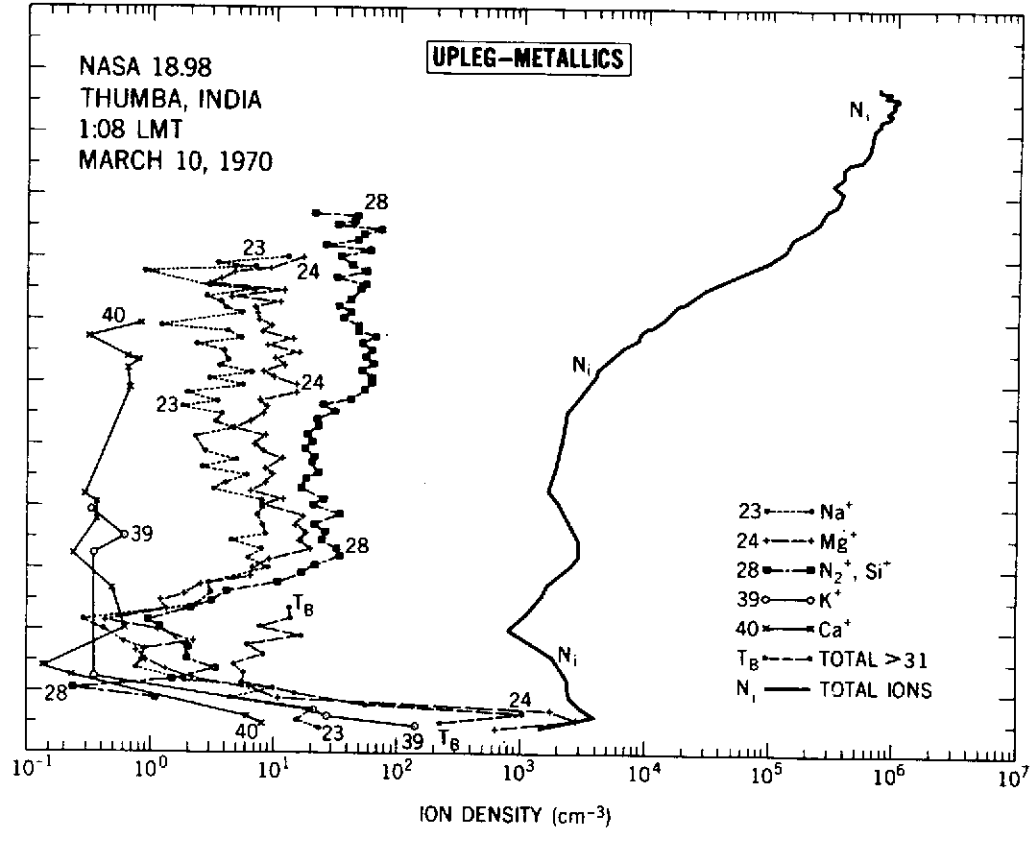
UPLEG–METALLICS
NASA 18.98
THUMBA, INDIA
1:08 LMT
MARCH 10, 1970
ION DENSITY (cm⁻³)
23 Na⁺
24 Mg⁺
28 N₂⁺, Si⁺
39 K⁺
40 Ca⁺
T_B TOTAL >31
N_i TOTAL IONS

Figure 3